Asphaltene Thermodynamic Precipitation during Miscible Nitrogen Gas Injection

Mukhtar Elturki, Missouri University of Science and Technology and Misurata University; and
Abdulmohsin Imqam*, Missouri University of Science and Technology

Summary

For many years, miscible gas injection has been the most beneficial enhanced oil recovery method in the oil and gas industry. However, injecting a miscible gas to displace oil often causes the flocculation and deposition of asphaltenes, which subsequently leads to a number of production problems. Nitrogen gas (N_2) injection has been used to enhance oil recovery in some oil fields, seeking to improve oil recovery. However, few works have implemented N_2 injection and investigated its effect on asphaltene precipitation and deposition. This research investigated the N_2 miscible flow mechanism in nanopores and its impact on asphaltene precipitations, which can plug pores and reduce oil recovery. First, a slimtube was used to determine the minimum miscibility pressure (MMP) of N_2 to ensure that all of the experiments would be conducted at levels above the MMP. Second, filtration experiments were conducted using nanocomposite filter membranes to study asphaltene deposition on the membranes. A filtration apparatus was designed specifically and built to accommodate the filter membranes. The factors studied include N_2 injection pressure, temperature, N_2 mixing time, and pore size heterogeneity. Visualization tests were conducted to highlight the asphaltene precipitation process over time. Increasing the N_2 injection pressure resulted in an increase in the asphaltene weight percent in all experiments. Decreasing the pore size of the filter membranes increased the asphaltene weight percent. More N_2 mixing time also resulted in an increase in asphaltene weight percent, especially early in the process. Visualization tests revealed that after 1 hour, the asphaltene particles were conspicuous, and more asphaltene clusters were found in the test tubes of the oil samples from the filter with the smallest pore size. Chromatography analysis of the produced oil confirmed the reduction in the asphaltene weight percent. Microscopy and scanning electron microscopy (SEM) imaging of the filter membranes indicated significant pore plugging from the asphaltenes, especially for the smaller pore sizes. This research highlights the severity of asphaltene deposition during miscible N_2 injection in nanopore structures so as to understand the main factors that may affect the success of miscible N_2 injection in unconventional reservoirs.

Introduction

The gas injection method has become a widespread technology to improve oil production in unconventional shale reservoirs in the United States. Although hydraulic fracturing technology in horizontal wells can be used to retrieve trapped oil, only 4 to 6% can be recovered (Biheri and Imqam 2020, 2021a, 2021b; Elturki et al. 2021). Very recently, gas injection methods have been studied in unconventional shale reservoirs using N_2 and carbon dioxide (CO_2) injection, and the results have demonstrated a positive impact on increasing oil recovery (Elwegaa and Emadi 2019; Altawati et al. 2020). Multiphase flow production has the potential to cause many issues in the oil industry; the multiphase fluids (i.e., gas, oil, condensate, and water) together with scales can cause some problems including wax and asphaltene deposition, formation of hydrates, slugging, and emulsions (Shi et al. 2021). Deposition of organic hydrocarbon solids in oil and gas reservoirs could cause many flow assurance problems during the oil and gas production process. These materials could increase the flow resistance and disrupt production or even plug the pipelines (Hassanpouryouzband et al. 2020; Ali et al. 2021). One of the major problems during gas injection in unconventional reservoirs could be asphaltene deposition and precipitation. Asphaltene, a solid component of crude oil, has an extremely high molecular weight (Mozaffari et al. 2015; Rashid et al. 2019). Asphaltene can be found in colloidal suspensions or in solution under reservoir pressure and temperature conditions (Jamaluddin et al. 2002). Asphaltene instability can be induced when the solubility of heavy components changes during the gas injection process (Fakher and Imqam 2019). Changes in temperature, pressure, and crude oil composition in a reservoir will result in the precipitation of asphaltene on solid surfaces during oil flows from the reservoir to the surface (Kar et al. 2020). As a consequence, asphaltene aggregates and nanosized particles can form clusters that may cause critical issues by blocking wellbore pores and production facilities (Alves et al. 2019). CO_2 and N_2 could cause a different degree of asphaltene flocculation into the reservoir. CO_2 has good solubility in crude oil and can easily attain a supercritical condition in reservoir conditions (Wang et al. 2018). For dead oils, CO_2 solubility ranges from 0.100 to 0.800 (mole fraction) for low and high temperatures, respectively (Nguyen and Ali 1998; Mahdaviara et al. 2021). On the other hand, the CO_2 solubility of live oils ranges from 0.062 to 0.966 (mole fraction) for low and high temperatures, respectively (Rostami et al. 2017). Thus, the mass transfer ability of supercritical CO_2 is strong. In the CO_2 injection process, the CO_2-crude oil system could easily reach a miscible or near-miscible state that enhances extraction of the light hydrocarbon components from crude oil into the gas phase. At similar thermodynamic conditions, N_2 has weaker solubility in crude oil than CO_2. N_2 has a weak mass transfer capacity, which could lead to the poor extraction of light hydrocarbons and probably less asphaltene flocculation compared to CO_2 (Chung 1992; Wang et al. 2018).

Recently, many experimental studies have examined the effect of gas injection, including CO_2 and N_2, on the stability of asphaltene in a crude oil system (Jamaluddin et al. 2002; Moradi et al. 2012a; Buriro and Shuker 2012, 2013; Soroush et al. 2014; Alimohammadi et al. 2017; Alves et al. 2019; Fakher and Imqam 2020; Afra et al. 2020; Kar et al. 2020; Elturki and Imqam 2020a, 2021a). Jamaluddin et al. (2002) combined various molar concentrations of N_2 with the reservoir fluid to investigate the instability of asphaltene. Their results showed that raising the concentration of N_2 increased the instability of asphaltene and also expanded the bulk precipitated amount. Moradi et al. (2012a) used natural depletion and N_2 injection processes to study the instability of asphaltene aggregates. N_2 produced an extreme negative alteration in the asphaltene instability, especially for heavier crudes. They also stated that the evaporation of N_2 improved the capability of oil to overcome the association of the flocs and breakdown the complex clusters. Soroush et al. (2014) investigated the effect of miscible and immiscible CO_2 flooding on the damage to porous media. They concluded that (1) when the

*Corresponding author; email: aimqam@mst.edu

Original manuscript received for review 29 June 2021. Revised manuscript received for review 23 August 2021. Paper (SPE 208588) peer approved 30 August 2021.

MMP is greater than that of CO_2, the trapped gas in porous structures could reduce the permeability; and (2) the pore plugging was much more severe compared to conditions below the MMP. On the other hand, asphaltene deposition was the principal factor in reducing the permeability during miscible injection pressure. Alves et al. (2019) researched the effect of temperature on asphaltene precipitation and concluded that when the temperature rose, the asphaltene precipitation decreased. Afra et al. (2020) studied the effect of CO_2 injection on the structure and the stability of asphaltene using four crude oil samples. Their work using infrared spectroscopy and acid/base identification demonstrated that asphaltene stability was disturbed when the amine group of one of the tested asphaltene samples could form an amide functional group by reacting with CO_2. Fakher and Imqam (2020) conducted experiments investigating asphaltene deposition in different pore sizes under various conditions. They concluded that asphaltene caused severe problems in both conventional reservoirs with large pores and unconventional reservoirs with nanopores. They also stated that as the oil viscosity increased, the asphaltene concentration rose as well. Kar et al. (2020) performed static vial tests and dynamic flow tests using six nonionic, weakly ionic, and ionic surfactants to study the effect of various surfactants on removing the deposited asphaltene on the surface of flowlines. Their results demonstrated that all surfactants removed the deposited asphaltene with less severe asphaltene aggregation. Additionally, the ionic surfactants were found to be the most effective chemical in asphaltene deposition removal. Injection of CO_2 and N_2 mixtures has been studied for storing CO_2 and increasing hydrocarbon production from unconventional resources (Hassanpouryouzband et al. 2018b, 2019). They investigated the CO_2 capture efficiency at various injection pressure, and the results demonstrated that the efficiency of CO_2 capture depends on the reservoir conditions such as pressure and temperature. The results also showed that there is an optimal reservoir pressure for a given reservoir temperature at which the maximum volume of CO_2 can be extracted from the injected flue gas or CO_2-N_2 mixtures.

Few studies have investigated the negative effects of asphaltene deposition and precipitation on pore plugging in unconventional reservoirs. Moradi et al. (2012b) conducted an experiment using N_2 and methane with a 0.2-μm-pore size filter membrane and reported that the asphaltene deposition was much higher when using methane than with N_2. Shen and Sheng (2018) studied the asphaltene aggregates precipitated during CO_2 and methane injection in shale oil samples. They used different filter membranes (i.e., 200, 100, and 30 nm) to investigate asphaltene deposition. Their study of coreflooding concluded that the oil recovery decreased because of the increase in asphaltene precipitation and deposition. Elturki and Imqam (2020b) conducted experiments during immiscible N_2 injection into nanoshale pore structures to investigate the instability of asphaltene. Various parameters were selected and examined, including temperature, pressure, and mixing time. They concluded that higher pressure resulted in a higher asphaltene weight percent, especially in smaller pore size structures, but the temperature had the opposite effect. Fakher and Imqam (2019) conducted experiments using nanocomposite filter membranes to investigate asphaltene precipitation during CO_2 injection. Their study concluded that oil recovery was enhanced when increasing the pore size; thus, the asphaltene weight percent decreased. Also, their study showed an increase in oil recovery with an increase in the asphaltene weight percent when the injection pressure was raised. However, a literature review found limited investigations of the factors impacting asphaltene deposition during N_2 injection, especially in nanopore reservoirs.

Even though there are many studies on the thermodynamic behavior of asphaltene precipitation during CO_2 injection, the structure and chemistry of the asphaltene reaction with N_2 remains poorly investigated and understood, especially in unconventional shale reservoirs. This research extends the previous work conducted by Elturki and Imqam (2021b), which investigated the impact of immiscible N_2 injection on asphaltene precipitation. The present research aimed to investigate the severity of asphaltene damage, especially in nanopore structures present in unconventional reservoirs. Asphaltene precipitation and deposition due to miscible N_2 injection in the nanopores was studied, and the asphaltene weight percent was quantified in all experiments. By studying the impact of various factors on asphaltene formation damage, asphaltene deposition may be mitigated in future applications of N_2 injections.

Asphaltene Definition and Precipitation Mechanism

Asphaltene is one of the most complex solid components comprising crude oil. Asphaltene can be defined as "the heaviest component of petroleum fluids that is insoluble in light *n*-alkanes such as *n*-pentane or *n*-heptane, but soluble in aromatics such as toluene" (Goual 2012). The main components of crude oil are saturates, aromatics, resins, and asphaltenes (Fakher and Imqam 2020). All of these components are held together with resins that have both polar and nonpolar sites, making resins a perfect connector between all of the components. As conditions change, the forces that bind all of the components become weaker and more severe; thus, the asphaltene starts to precipitate. The common conditions that may change include pressure; temperature; solvent injection, such as CO_2; and a high oil production flow rate (Bahman et al. 2017). High-density asphaltene flocculation starts to form after the precipitation, if the conditions are suitable. This flocculation will start to deposit in the pores of the reservoirs (Srivastava and Huang 1997), with buildups forming if an excessive deposition occurs, causing pore plugging. **Fig. 1** shows the main alterations that can occur because of asphaltene deposition, including pore plugging, adsorption of the asphaltene to the rock grains, and changes in wettability (Fakher 2020).

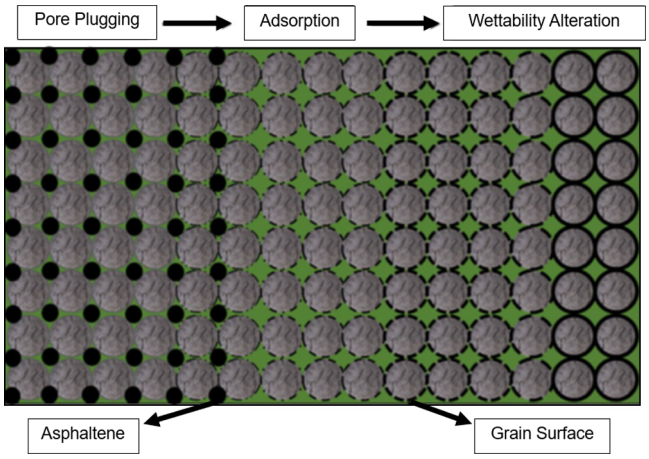

Fig. 1—Asphaltene impacts on oil recovery (Fakher 2020).

Experimental Design

Fig. 2 shows the experimental flow chart for the three types of experiments that were conducted: (1) MMP determination, (2) filtration, and (3) asphaltene visualization. First, the MMP of N_2 was determined to ensure the pressure in the filtration experiments fell within miscible conditions. Then, the visualization experiments were conducted, after which the asphaltene weight percentages were calculated. Chromatography analysis of crude oil confirmed the change in the asphaltene weight percent after the filtration experiments compared to the original crude oil. Microscopy imaging was used to highlight the effect of the asphaltene deposition into the pores of the filter membranes.

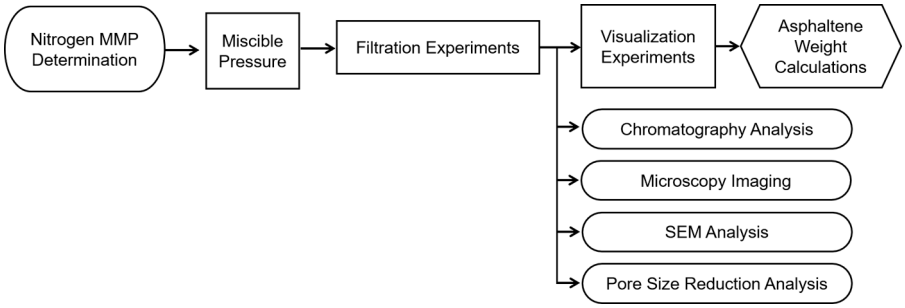

Fig. 2—Experimental design flow chart.

Experimental Material and Description. The experimental materials included the following elements.

Crude Oil. Crude oil with a viscosity of 19 cp, a density of 0.864 g/cm^3, and a gravity of 32 °API was used. The viscosity was measured using a rheometer. Gas chromatography-mass spectrometry determined the composition of the crude oil, as shown in **Table 1.**

Component	Weight percentage (%)
C8	64.55
C9	0.28
C14	0.31
C15	0.35
C16	0.43
C17	3.92
C18	0.20
C19	1.17
C20	3.60
C21	0.93
C22	2.66
C24	1.97
C27	5.94
C28	7.22
C29	1.32
C30+ (including asphaltene)	5.17
Total	100

Table 1—Crude oil composition.

Filter Membranes. Various sizes of filter membranes (i.e., 50, 100, and 450 nm) were used to investigate the effect of different pore sizes. The selection of filter membrane pore sizes was based on the pore size distribution of shale reservoirs, specifically Eagle Ford (Shen and Sheng 2017). The membranes were cut to the desired shape based on the 45-mm diameter of the filtration vessel.

Specially Designed High-Pressure High-Temperature Filtration Vessel. A high-pressure high-temperature filtration vessel was designed specifically to accommodate filter paper membranes for oil filtration experiments. The filtration vessel had a length of 15.24 cm with inside and outside diameters of 5 and 7.62 cm, respectively.

Nitrogen. An N_2 gas cylinder with 99.9% purity was connected to the filtration vessel and used for the N_2 injection. A pressure regulator controlled the N_2 cylinder pressure.

Oven. An oven with enough space to accommodate the filtration vessel was used to investigate the effect of various temperatures on asphaltene precipitation and deposition during N_2 injection. The oven was manufactured by Despatch (Model LBB2-27-2, chamber dimensions: 94 cm wide × 94 cm deep × 89 cm high).

n-Heptane. This solvent was used to dissolve the oil samples in the tubes to quantify the asphaltene weight percent after each experiment.

Slimtube. A stainless steel slimtube packed with sand was used to determine the MMP of N_2. The slimtube had a weight of 2211 g with a length of 13.1 m (inside and outside diameters were 0.21 and 0.41 cm, respectively).

A summary describing all of the experiments conducted in this research and the significant factors that were investigated are presented in **Table 2.**

No.	Experiment/Analysis	Factor Studied	Factor Value	Pressure
1	MMP	Temperature	32 and 70°C	
2	Filtration	Temperature	32, 70, and 90°C	1,750 psi
3		Mixing time	10, 60, and 120 min	1,750 psi
4		Injection pressure/heterogeneity	450, 100, and 50 nm	1,750, 2,000, and 2,250 psi
5			100, 100, and 100 nm*	1,750, 2,000, and 2,250 psi
6	Visualization	Mixing time	10, 60, and 120 min	1,750 psi
7		Injection pressure/heterogeneity	450, 100, and 50 nm	1,750 and 2,250 psi
8			100, 100, and 100 nm*	2,000 psi
9	Microscope imaging	Pore size plugging	450, 100, and 50 nm	1,750, 2,000, and 2,250 psi
10	SEM analysis	Pore size plugging	450, 100, and 50 nm	1,750 and 2,250 psi
11	Gas chromatography	Chemical structure	1,750 and 2,250 psi	1,750 and 2,250 psi
12	Pore plugging	Pore size distribution	450, 100, and 50 nm	1,750 and 2,250 psi

*Uniform pore size distribution.

Table 2—Summary of all experiments conducted in this research.

MMP Experiment. To ensure that all of the filtration experiments would occur at a level higher than the MMP, experiments were initially conducted to determine the MMP. The MMP can be defined as the lowest pressure at which a gas can create miscibility with the reservoir oil at the reservoir temperature. In other words, the MMP is the lowest pressure at which miscibility between the injected gas and reservoir oil is achieved when the interfacial tension between the oil and gas disappears after multiple contacts. **Fig. 3** shows a schematic diagram of the slimtube experimental setup. The main components of the MMP experiment included a syringe pump, three accumulators, gas cylinders, a stainless steel slimtube packed with sand, and a backpressure regulator. The first step was a pretest to calculate the pore volume (PV). In the second step, the slimtube was filled with the crude oil at a low rate of 0.5 PV to ensure that the slimtube was 100% saturated at the end of pumping. The final step involved experimental manipulation, whereby the temperature was adjusted to a predefined level, the gas cylinder was filled with N_2, and gas was pumped at a rate of 1.2 PV of gas injected. A backpressure regulator was installed at the outlet of the slimtube and used to adjust the pressure by using another water pump as a backpressure reservoir.

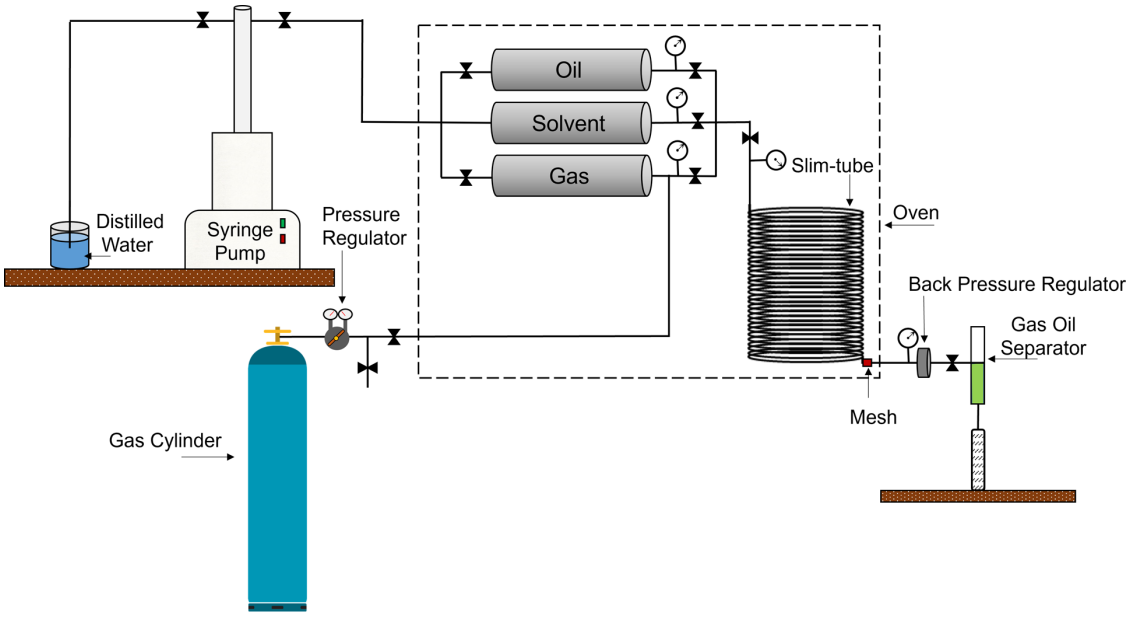

Fig. 3—Main components of the slimtube experimental setup.

MMP Experiment Procedure. First, the slimtube was fully saturated with the distilled water. Then, the oil was injected into the slimtube unit until fully saturated. This can be observed at the outlet of the slimtube when the produced liquids are only oil and thus ensure the slimtube is fully saturated. During all the experiments, the backpressure regulator was placed at the outlet with the desired pressure. The gas accumulator was filled with N_2. Then, N_2 was injected at a rate of 0.25 mL/min. Each experiment was stopped when

1.2 PV of gas was injected or when the gas broke through. The effluent was used to collect the produced oil. The MMP can be determined by plotting N_2 injection pressures vs. cumulative oil recoveries. Finally, the solvent of xylene was used after each experiment to clean the slimtube setup and to make sure there was no oil left in the slimtube that may affect the next experiment.

Filtration Experiments. The components of the filtration setup are shown in **Fig. 4.** The main components included a high-purity N_2 with a pressure regulator to control the pressure from the cylinder. The high-pressure high-temperature filtration vessel was designed to accommodate three mesh screens to support the filter membranes and prevent them from folding under high pressure. The mesh screens were designed with small holes that allowed the oil to pass through easily. Spacers between each mesh screen were added to support each mesh screen in its place, and rubber O-rings were used above and below each spacer to prevent leakage and to ensure that the oil and gas would pass through the filter paper membranes. A backpressure regulator was installed at the outlet of the filtration vessel and used to adjust the pressure in the syringe pump. The produced oil was collected using an effluent below the filtration vessel for further analysis. An oven controlled the temperature of the filtration vessel to study the effect of different temperatures. Finally, two transducers were installed at the inlet and outlet of the filtration vessel and were connected to a computer to monitor and record the pressure differences.

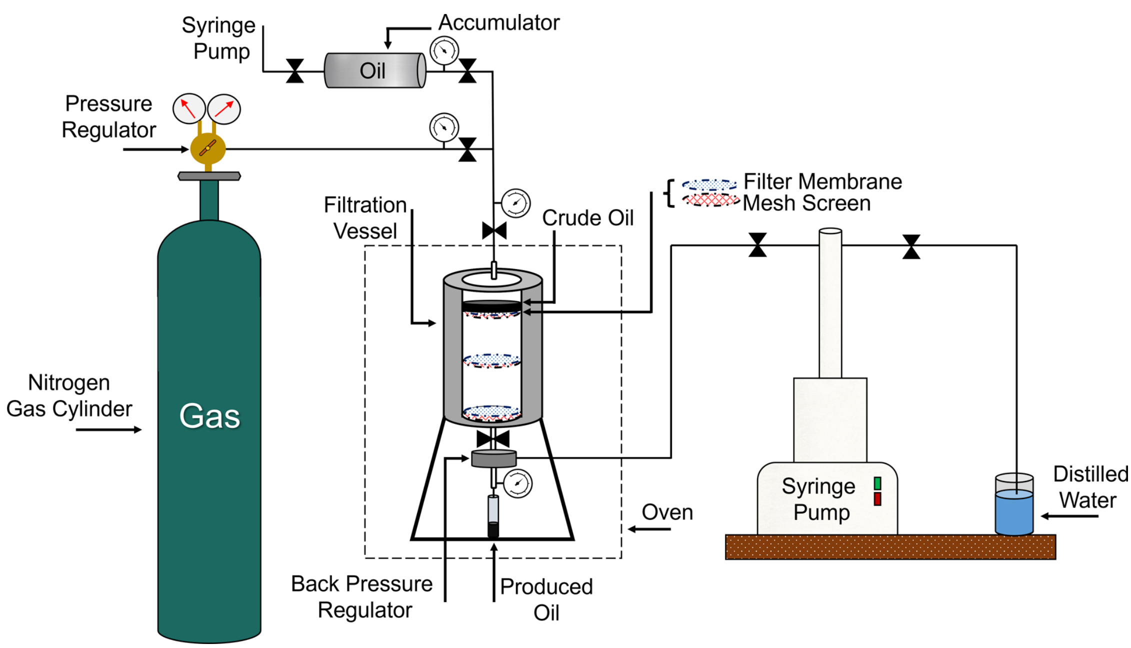

Fig. 4—Filtration experimental setup.

Filtration Experimental Procedure. The first set of mesh screens along with a filter membrane paper, rubber O-ring, and spacer were placed inside the filtration vessel, in that order. This step was repeated with the next two sets, after which the vessel was closed using a specially designed cap that ensured a tight connection between all of the sets and prevented leakage during the experiment. An oil accumulator was injected with 30 mL of crude oil into the vessel using a syringe pump. Next, the N_2 cylinder injected gas into the vessel to the desired level and exposed the crude oil to the gas for a specific mixing time. Then, the syringe pump at the outlet was turned to constant pressure but was adjusted to the required backpressure for each experiment to let the crude oil pass through the membranes. N_2 was injected continuously into the vessel, and the produced oil was collected for further analysis (e.g., chromatography analysis). The experiment was stopped when no further oil production was observed. During the experiment, the inlet and outlet pressures were recorded using transducers connected to a computer. The difference between the two pressures did not exceed 50 psi. After the experiment, the vessel was opened, and the remaining crude oil was collected from each filter membrane for analysis. Finally, the solvent *n*-heptane was used to clean the vessel, mesh screens, and spacers from oil in preparation for the next experiment.

Asphaltene Visualization Experiment Procedures. Asphaltene visualization experiments provide evidence of how asphaltene behaves in terms of precipitation and deposition at various conditions. These experiments were conducted to visualize the asphaltene precipitation and deposition using the following procedure:

1. In a test tube, 1 mL of crude oil collected from all filter membranes was combined with the produced oil and the remaining oil from the filtration experiments. The oil was collected using a pipette to ensure the accuracy of all samples.
2. Then, 40 mL of *n*-heptane was added to each test tube. Tubes were closed tightly to prevent *n*-heptane evaporation.
3. Each test tube was shaken well to ensure that the *n*-heptane was well dispersed within the crude oil.
4. A special laboratory stand was used to handle all of the test tubes. The asphaltene then started to settle slowly.
5. Photos were taken at specific time points (i.e., 0, 2, 4, and 12 hours) to observe the changes in asphaltene settling over time.

Asphaltene weight percent can be calculated by weighing the filter paper before and after the filtration process. The difference between these weights determines the asphaltene weight percent using the following equation:

$$\text{Asphaltene wt\%} = \frac{wt_{asphaltene}}{wt_{oil}} * 100, \quad (1)$$

where asphaltene wt% is the asphaltene weight percent, $wt_{asphaltene}$ is the asphaltene weight on the filter paper, and wt_{oil} is the oil sample weight. The asphaltene quantification test procedure is summarized in a flow chart in **Fig. 5.**

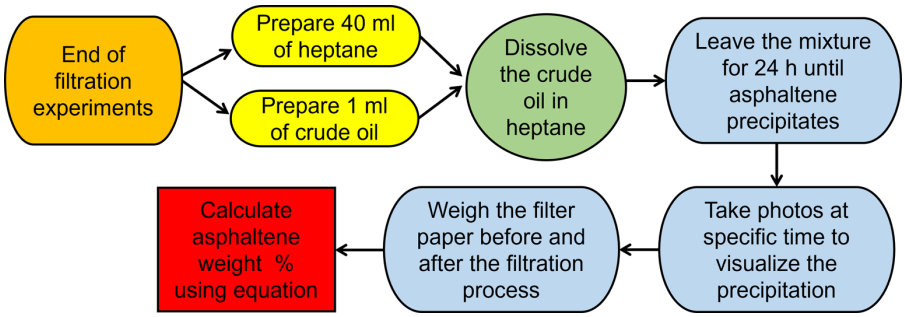

Fig. 5—Flow chart highlighting the main steps of asphaltene quantification.

Results and Discussion

MMP Experimental Results. The MMP experiments were conducted to ensure that all of the filtration experiments would occur at levels greater than miscible gas injection conditions. Crude oil with a viscosity of 19 cp, a density of 0.864 g/cm^3, and a gravity of 32 °API was used. The effect of temperature was studied on the MMP of N_2 to ensure that the miscible injection pressure was still achievable during the high pressure of the filtration experiments. To determine the MMP, the tested N_2 injection pressures were plotted vs. oil recoveries at 1.2 PV of gas injected or at gas breakthrough. The MMP can be estimated when the cumulative oil recovery is greater than or equal to 90% of the original oil in place. The solid lines in **Fig. 6** were used to determine the sudden slope change point in the measured oil recovery vs. injection pressure. The intersection point can be used to determine the MMP. The results demonstrated that with increasing temperature, the MMP decreased. This is the opposite of what occurs with a CO_2 MMP. The MMP of N_2 at 32°C was 1,600 psi, while at the higher temperature of 70°C, the MMP of N_2 was 1,350 psi, as shown in Fig. 6. Various studies stated that the MMP can increase or decrease depending on the oil composition (Sebastian and Lawrence 1992; Vahidi and Zargar 2007; Belhaj et al. 2013). Therefore, the results of this research can be explained by the fact that the temperature is inversely proportional to the N_2 MMP because of the N_2 remaining in the gaseous phase at the same conditions. Consequently, the effect of temperatures higher than 32°C were investigated in this research because miscibility can be achieved at higher temperatures.

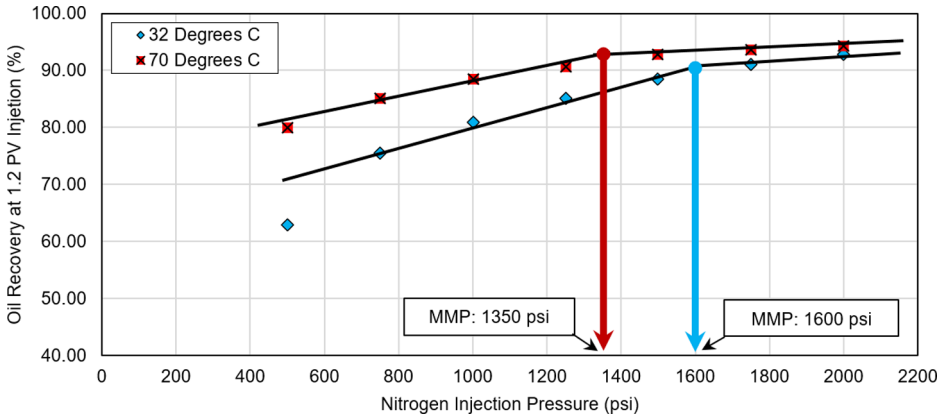

Fig. 6—N_2 MMP determination using an oil viscosity of 19 cp at 32 and 70°C.

Filtration and Visualization Results. ***Effect of Miscible Pressure Using Uniform Membrane Distribution.*** Three 100-nm filter membranes were placed in the filtration vessel to investigate the effect of using the same pore size structure and to compare the results to those using a heterogeneous distribution. A uniform distribution means that filter membranes of the same pore size were used. **Fig. 7** illustrates the paper membrane distribution inside the vessel. N_2 pressures of 1,750, 2,000, and 2,250 psi and a temperature of 32°C were used throughout these experiments.

Fig. 8 shows the asphaltene weight percent vs. N_2 injection pressure when using a uniform distribution. The results showed that the asphaltene weight percent was almost equal for most of the filter membranes used. At 1,750-psi injection pressure, the weight percent of asphaltene decreased slightly from 12.68% in the upper part of the 100-nm filter membrane to 12.07% in the lower part due to the asphaltene clusters having plugged the pores in the upper and middle areas of the 100-nm filter membrane. This prevented some oil from passing through and thus reduced the asphaltene percent in the lower part of the filter membrane. However, this did not occur when using 2,000-psi injection pressure, at which the asphaltene weight percent increased slightly from 13.6 to 13.80% in the upper and lower parts of the 100-nm filter, respectively. These observations demonstrated that the asphaltene clusters passed through all the filter membranes with approximately the same behavior at all the injection pressures studied. The asphaltene particles greater than 100 nm precipitated on the upper portion of the filter membrane, while the smaller particles passed through all the filters and reached the outlet with the produced oil. The slight fluctuation in the asphaltene weight percent occurred because some of the asphaltene clusters plugged some pores in the middle or lower filter membranes. The flow of oil inside the vessel was not smooth in all of the filter membranes because the pore plugging could not be controlled. The lowest amount of asphaltene was also found in the produced oil because of the pore plugging that resulted from the asphaltene clusters present throughout all the filter membranes.

A 2,000-psi N_2 injection pressure was selected to investigate the asphaltene precipitation over time. **Fig. 9** shows the asphaltene visualization process along a uniform membrane pore size distribution. At zero elapsed time, no asphaltene was observed, and the crude oil sample was entirely dissolved in *n*-heptane. After 1 hour, asphaltene started to form and precipitate, and suspended particles could

be seen in the uppermost section of the test tubes. The lower portion of the 100-nm filter exhibited slightly more suspended particles due to asphaltene plugging more pores in the upper and middle parts of the filter membranes. Over time, more asphaltene was deposited on the bottommost section of the test tubes. The visualization tests showed that most of the asphaltene particles formed and were deposited over 1 to 4 hours. Finally, after 12 hours, most of the asphaltenes were deposited, and few particles could be found in the supernatant. These results indicate that the asphaltene amount in all the filter membranes using the uniform distribution was almost equal in all of the 100-nm filters used. This confirms the results of the filtration experiment, which showed the same trend.

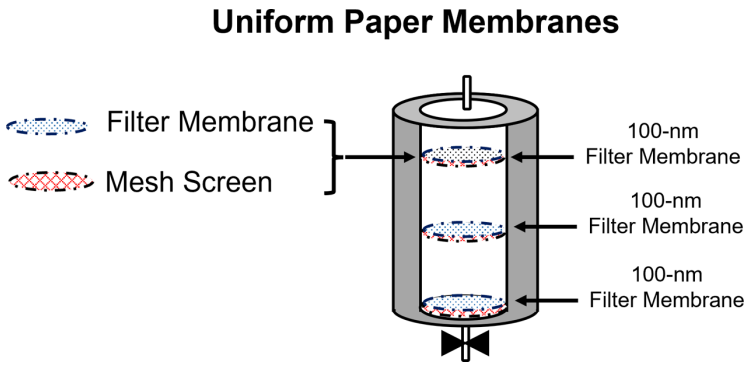

Fig. 7—Illustration of the uniform paper membrane distribution inside the vessel.

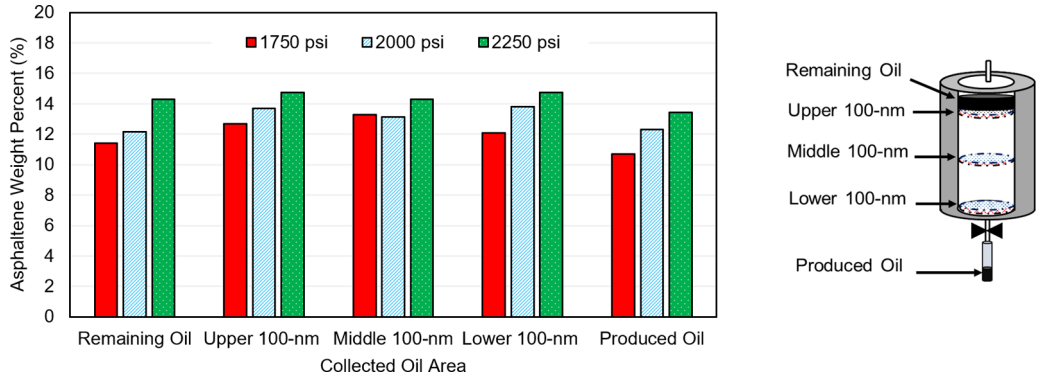

Fig. 8—Asphaltene weight percent distribution using uniform paper membranes with N_2 injections at 1,750, 2,000, and 2,250 psi.

Effect of Pore Size Heterogeneity. Three miscible N_2 pressures were investigated (i.e., 1,750, 2,000, and 2,250 psi) at 32°C with a 2-hour mixing time. The mixing time effect will be presented in the following sections. A heterogeneous condition of the filter membranes was examined, starting with a 450-nm filter in the upper mesh screen, 100-nm filter in the middle, and 50-nm filter in the lower mesh screen, as shown in **Fig. 10.** Increasing the pressure resulted in an increase in the asphaltene weight percent because the asphaltene resins connect all the solid components in crude oil that break down; thus, asphaltene levels will increase.

Fig. 11 presents the asphaltene weight percent using a heterogeneous paper membrane distribution during various N_2 injection pressures. When using 1,750-psi gas injection, the asphaltene weight percent increased significantly, from 11.67 to 17.33% in the 450- and 50-nm filters, respectively. This indicated that the asphaltene particles and clusters were affected by the injected pressure, which resulted in asphaltene deposition depending on the asphaltene particle size. This led to plugged pores in the filter membranes, especially in the 50-nm filter. The ability of asphaltene particles to pass through the filter membranes was affected by the size of their pores. As a result of Brownian motion, the asphaltene aggregates continued to interact with one another, forming larger particles. Because of the large radial diffusivity of the particles, smaller aggregates have a higher tendency to deposit (Hassanpouryouzband et al. 2018a). These observations strongly indicated that the asphaltene had altered the ability of the oil to pass through, which can occur in real reservoirs, causing severe problems. The produced oil had a lower asphaltene weight percent because of the asphaltene clusters having plugged the pores in all the filter membranes. Also significant is that when the filtration vessel was opened to collect the crude oil, the volume of the oil had increased, and bubbles could be seen in the oil. This can be explained by the pressure increase, which made the N_2 more soluble in the oil; thus, the oil swelled. This phenomenon resulted in a slight decrease in the N_2 pressure inside the vessel. The N_2 started to be liberated from the oil after the pressure was relieved. Finally, the oil returned to its original volume. **Fig. 12** shows the bubbles that formed in the oil when it was collected from the filtration vessel.

The visualization of the asphaltene deposition process over time was implemented by analyzing the collected oil after concluding each experiment. The oil collected from 450-, 100-, and 50-nm filter membranes was analyzed under 1,750-, 2,000-, and 2,250-psi N_2 injection pressures. Test tubes were used to mix the oil samples with the solvent *n*-heptane at a ratio of 1:40. Four times were selected (i.e., 0, 1, 4, and 12 hours) to investigate and visualize the asphaltene deposition process. The photos illustrate that at 0 hours, all the test tubes held oil that was fully dissolved in *n*-heptane, and no asphaltene was observed during all the selected injection pressures using any of the filter membranes. After 1 hour, it was observed that asphaltenes started to form because the bonds between the asphaltene and resins were weakened by pressure. Interestingly, the image of the 50-nm filter showed a slightly higher amount of suspended asphaltenes during the 1,750-psi gas injection because the smaller pore size trapped more particles of asphaltene, as shown in **Fig. 13.** This observation also occurred during the 2,000-psi gas injection, but not at 2,250 psi.

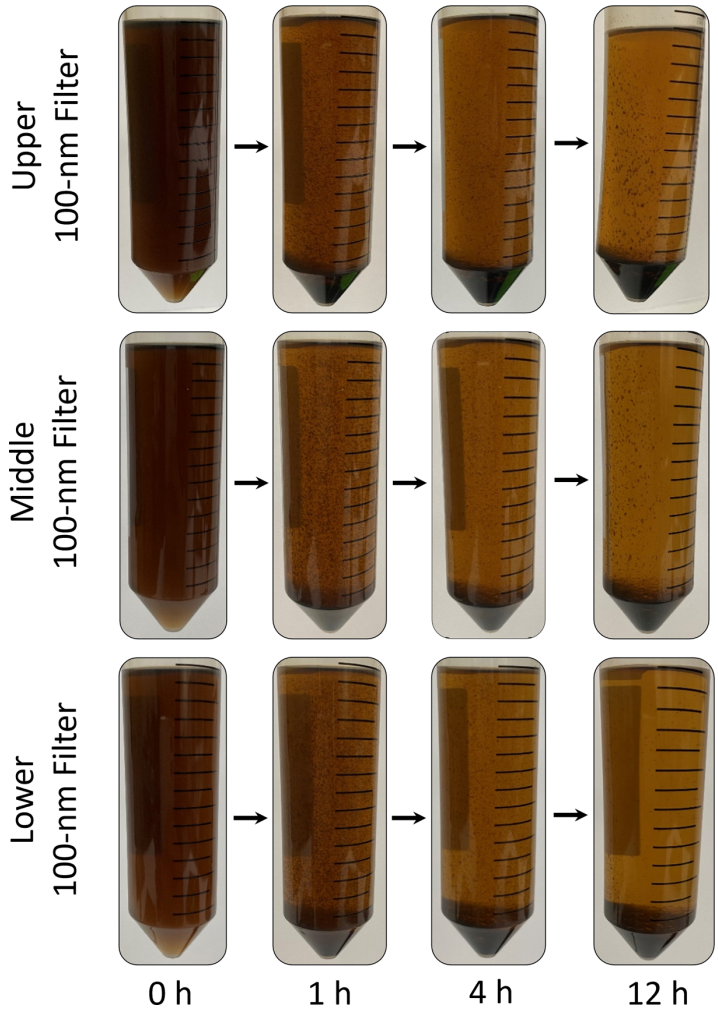

Fig. 9—Asphaltene precipitation and deposition visualization process using 2,000-psi injection pressure and a uniform distribution at 32°C with a 2-hour mixing time.

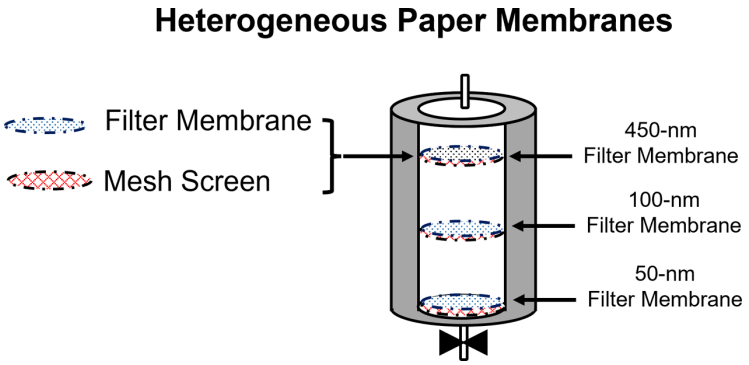

Fig. 10—Illustration of the heterogeneous paper membrane distribution inside the vessel.

During the highest pressure (2,250 psi), the asphaltene precipitated slightly faster than at the lower pressures, as shown in **Fig. 14.** Moreover, the asphaltene deposition and precipitation started after 1 hour, which can be observed at the bottommost section of the test tubes, because they became dark in color due to the high asphaltene concentration. After 4 hours, more asphaltene settled, and less asphaltene suspension was found in the supernatant. This observation was more obvious at the highest pressure condition of 2,250 psi. As time progressed, more asphaltene deposition was observed in all captured photos of all test tubes. After 12 hours of precipitation, the supernatant became lighter in color, but a darker color was still found in the bottom of all test tubes, representing asphaltenes. These results demonstrated that pressure has a significant effect on asphaltene instability. It is therefore important to analyze the pressure effect on the asphaltene stability to anticipate and avoid any related issues.

Effect of Mixing Time. The mixing time is the total time the oil was exposed to the desired N_2 pressure inside the reservoir cylinder and left at 32°C to allow the N_2 to mix well with the crude oil. Three different experiments with times of 10, 60, and 120 minutes were selected to investigate the effect of the mixing time on the asphaltene precipitation and deposition during 1,750-psi N_2 injection at a temperature of 32°C. **Fig. 15** shows the asphaltene weight percent in all filter membranes during various mixing times. The results

highlight that increasing the mixing time resulted in an increase in the asphaltene weight percent. For a 450-nm filter, the asphaltene weight percent increase ranged from 8.95 to 11.67% for 10 and 120 minutes, respectively. Decreasing the filter membrane size led to an increase in the asphaltene weight percent because of pore plugging from asphaltene clusters. A 10-minute mixing time had a lower effect on the asphaltene clusters because of the limited time for the gas to weaken the bonds between the asphaltene and resins. Given these observations, the mixing time has an effect on the instability of asphaltene aggregation. These data highlight that the mixing time has a crucial effect on the asphaltene deposition within 120 minutes, although this deposition may increase slightly over longer times, especially in smaller pores.

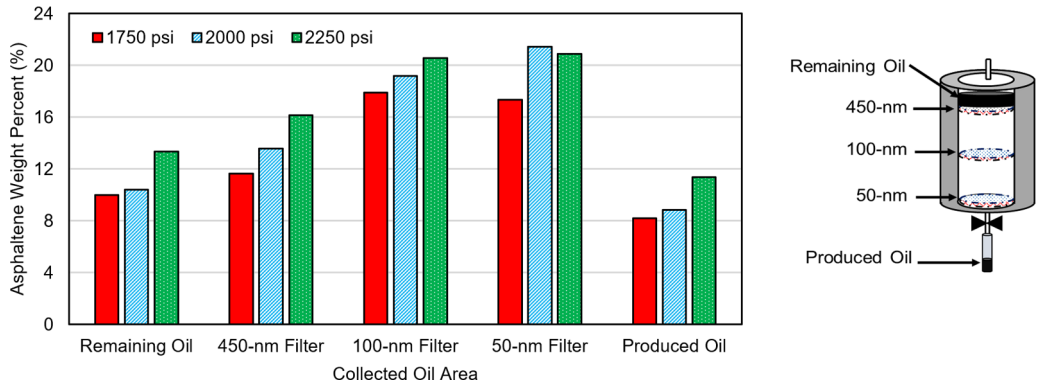

Fig. 11—Asphaltene weight percent using a heterogeneous distribution at 1,750-, 2,000-, and 2,250-psi N_2 injection.

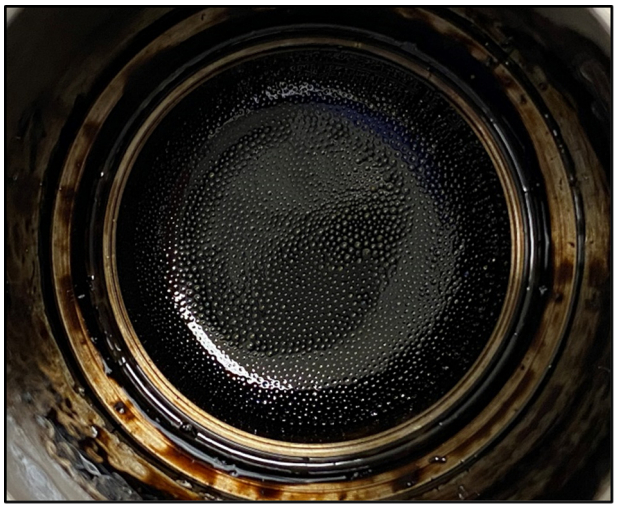

Fig. 12—N_2 dissolved in the crude oil being liberated at an injection pressure of 1,750 psi.

The remaining oil was collected from all of the filtration experiments and all mixing times. Every experiment was conducted at 1,750 psi and 32°C. **Fig. 16** shows the effect of a 1,750-psi N_2 injection on the remaining oil, using mixing times of 120, 60, and 10 minutes. Increasing the mixing time also increased the asphaltene precipitation process time. For 10 minutes of mixing time, the asphaltene deposition process was slower than for 60 and 120 minutes. This could result from the short time (10 minutes), during which the N_2 could affect the asphaltene instability; thus, there were fewer suspended asphaltene particles in the test tube, especially after 1 hour. After 4 hours, the bottommost section of the test tubes for the 120-minute mixing time became darker than during the 10-minute mixing time. This indicates that the asphaltene particles significantly aggregated during longer mixing times. For all mixing times, after 12 hours from the beginning of the experiment, most of the asphaltene particles had settled, although there were some suspended particles in the supernatant of the 60- and 120-minute mixing times. The prolonged interaction of the N_2 with the oil resulted in more asphaltene instability; thus, severe problems could occur in actual unconventional reservoirs.

Effect of Temperature on Asphaltene Deposition. Because the MMP of N_2 decreases as the temperature increases, the investigation of higher temperatures is achievable because miscibility will always occur with higher pressures when the temperature is high. Experiments were conducted at two temperatures (i.e., 70 and 90°C) to investigate the effect of a higher temperature on the asphaltene stability and to compare that with the experiment discussed earlier at 32°C. The 32°C represents room temperature, and 70°C represents the average temperature of shale basins. To ensure the stability of the required temperature, an especially designed vessel was placed inside the oven in both experiments. Both experiments used a pressure of 1,750 psi for N_2 injection, a heterogeneous filter membrane distribution, and a 2-hour mixing time. Increasing the temperature increased the asphaltene weight percent, as shown in **Fig. 17.** The results demonstrated that the highest asphaltene weight percent occurred on the 50-nm filter membranes due to their smaller-sized pores. The asphaltene weight percent decreased in the 50-nm filter from 14.28 to 11.59% for 70 and 90°C, respectively, compared to 17.33% for 32°C. In stable oils, the suspension colloidal particles of asphaltene were covered by resins that bind strongly with asphaltene. This connection between asphaltene and resins becomes stronger at higher temperatures, which keeps the asphaltene dissolved in oil (Hoepfner et al. 2013). At higher temperatures, a smaller amount of asphaltene colloidal will be produced, but it will tend not to

form strong associations because the colloids are dispersed effectively by resins (Branco et al. 2001). The precipitated asphaltenes that form from the colloidal suspension particles at higher temperatures tend to dissolve in the oil; thus, more asphaltenes will be produced in a soluble condition but fewer in colloidal conditions (Chandio et al. 2015). The resins have a tendency to self-associate, and that tendency is much stronger at lower temperatures. Therefore, the bond between the asphaltenes and resins becomes weaker (Pereira et al. 2007). Consequently, a higher amount of asphaltene precipitation can form because the molecules of asphaltene become stronger in terms of polarity, resulting in more aggregation at lower temperatures. Note that the membrane pore size had the same effect at both temperatures: As the filter paper membrane pore size decreased, the asphaltene weight percent increased. This is due to the asphaltene particle size plugging the pores much more in the 50-nm filter membrane, such that more asphaltene was observed. In all experiments, the asphaltene weight percent in the produced oil was the lowest because the asphaltene particles precipitated and plugged the nanopaper membranes gradually, which then reduced the amount of asphaltene in the oil outlet.

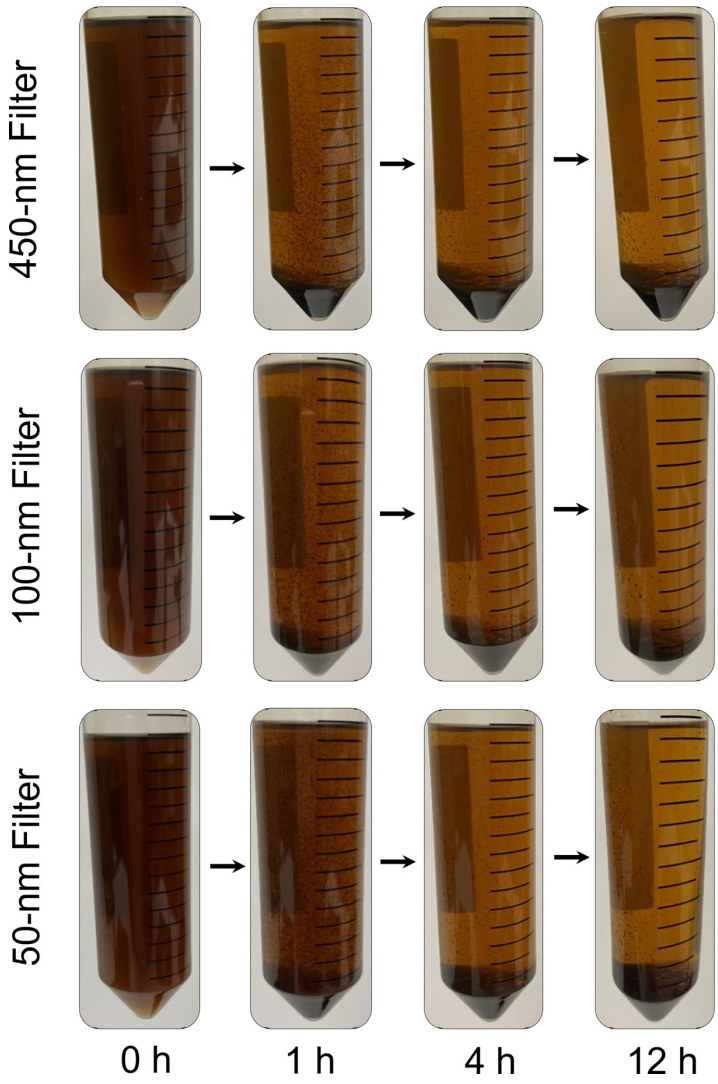

Fig. 13—Visualization of the asphaltene precipitation and deposition process at 1,750 psi using a heterogeneous distribution at 32°C.

Further Analysis and Discussion

Chromatography Analysis. The produced oil was collected from the gas injection filtration experiments. Then, gas chromatography-mass spectrometry (GC6890-MS5973) was used to identify the main chemical components and their presence, including asphaltenes. First, the original oil with 19 cp viscosity that was used in all experiments was analyzed, and its components were compared to the oil analysis after the experiments. Two pressures (i.e., 1,750 and 2,250 psi) were selected to investigate the chemical changes in the oil after the experiments, especially the heavy components of asphaltene. **Fig. 18** shows the distribution of oil components before and after N_2 gas injection filtration experiments at 1,750 and 2,250 psi. The results revealed that the asphaltene components decreased from 5.17 to 3.14% using 1,750 psi N_2 gas injection. This indicates that the filter paper membranes inside the filtration vessel reduced the ability of the asphaltene clusters to pass through; thus, the pores were plugged. This resulted in a decrease in the heavy components in the produced oil. Increasing the pressure to 2,250 psi resulted in more asphaltene components, with the analysis showing an increase from 3.14 to 3.91% when using 1,750 and 2,250 psi, respectively. This was because higher pressure will force more asphaltene clusters to pass through, thereby causing there to be a higher percent of asphaltene in the produced oil. **Table 3** presents the chromatography analysis of the original oil and the produced oil at 1,750 and 2,250 psi.

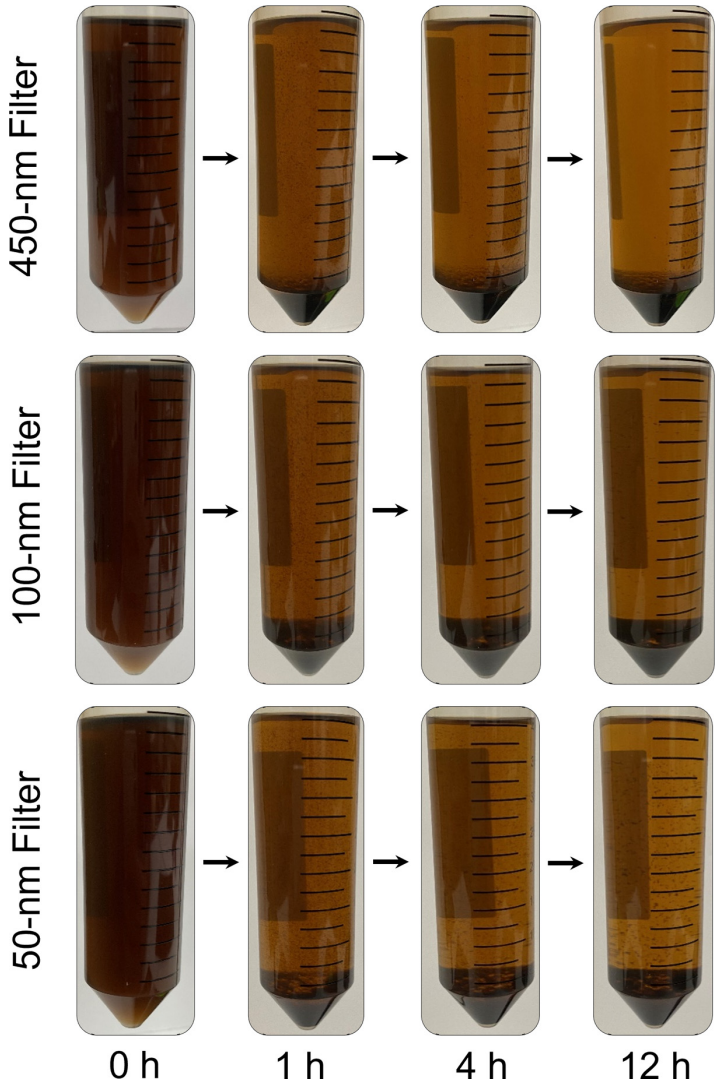

Fig. 14—Visualization of the asphaltene precipitation and deposition process at 2,250 psi using a heterogeneous distribution at 32°C.

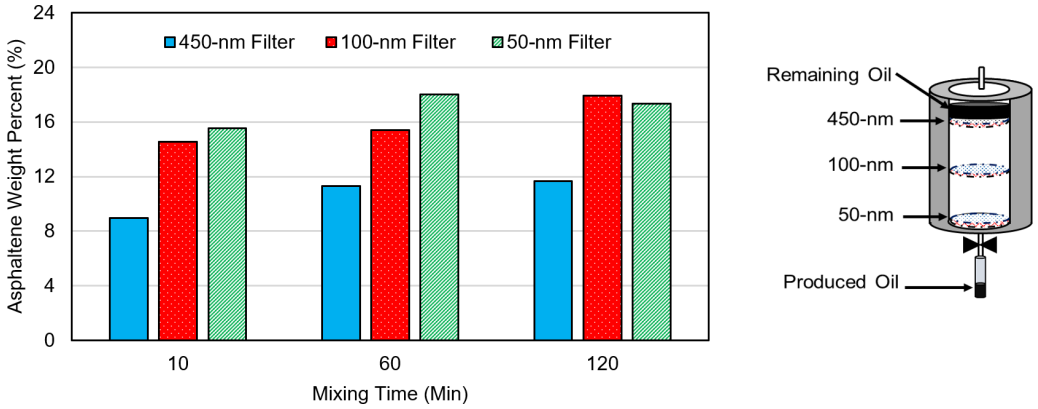

Fig. 15—Asphaltene weight percent at mixing times of 10, 60, and 120 minutes using 450-, 100-, and 50-nm filter membranes.

Microscopy Imaging Analysis. Asphaltene particles are induced by gas injection, and large asphaltene clusters can form, leading to asphaltene holdup in a reservoir. Asphaltene can plug the pores and cause severe problems, including a reduction in oil relative permeability, altering the wettability of the rock, and an overall reduction in oil production. The 450- and 50-nm filter paper membranes with a 2,000-psi gas injection were cleaned by the solvent *n*-heptane to highlight the pore plugging in the filter paper. **Fig. 19** shows the filter membrane before conducting the experiments, after conducting the filtration experiments, and after cleaning the crude oil from the filter membranes. The photo shows the asphaltene deposited in the filter membrane pores and the plugged path for the crude oil to move, especially in the 50-nm filter membrane, which had the smallest pore size.

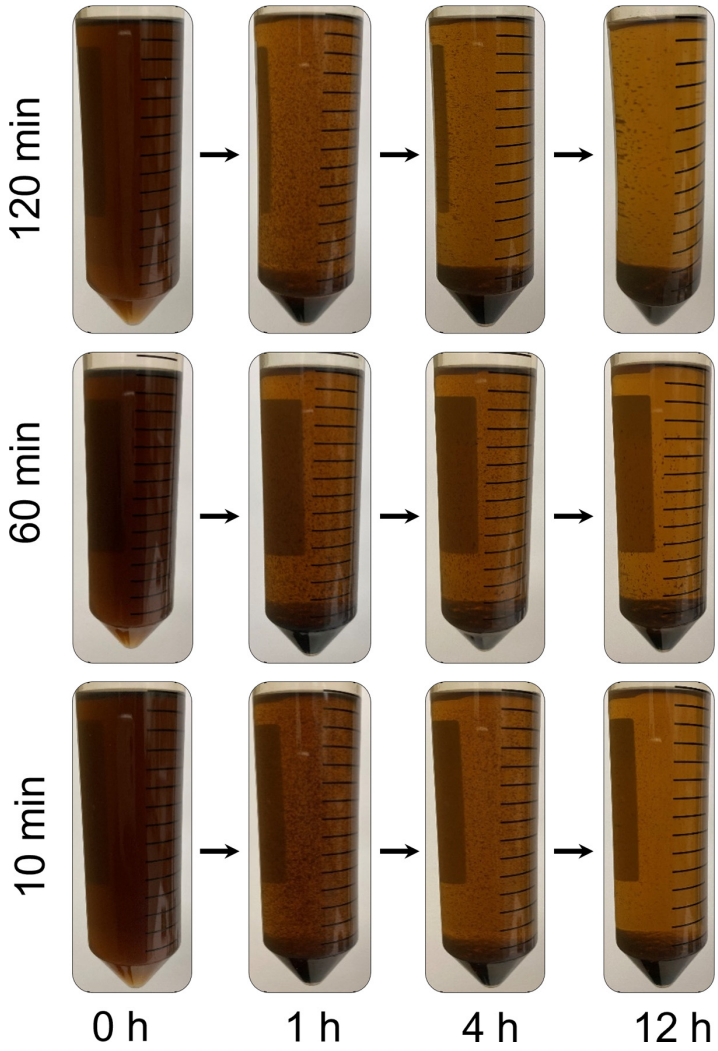

Fig. 16—Visualization of the asphaltene precipitation and deposition process at different mixing times.

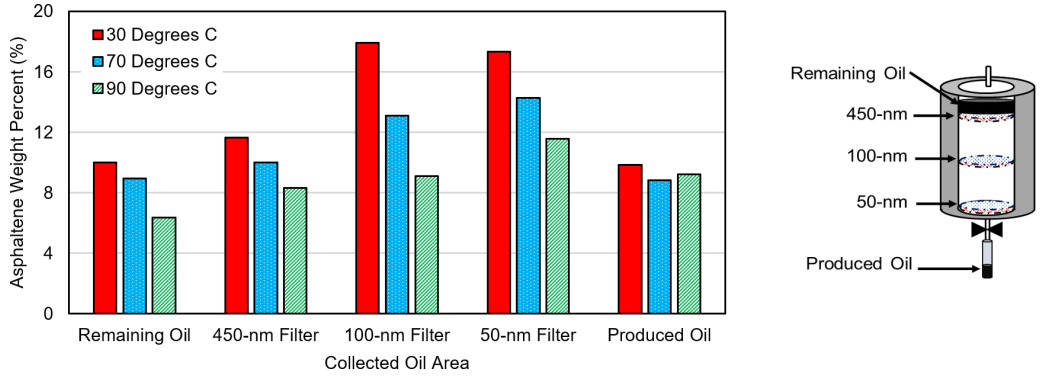

Fig. 17—Asphaltene weight percent using a heterogeneous distribution during N_2 injection at 1,750 psi at different temperatures.

A HIROX digital microscope was used to identify the plugged pores in the filter membranes. Showing the filter membranes' microstructure can highlight the severity of the asphaltene aggregation on different pore size structures. **Fig. 20** shows the microscopic images (20 μm) of the filter membranes' pore structure of the 450-, 100-, and 50-nm filters using a miscible N_2 injection pressure of 1,750, 2,000, and 2,250 psi at 32°C. The images were captured after cleaning and also after exposure to the filter membranes in an *n*-heptane solvent for 24 hours. Noticeable differences occurred in the aggregation of the precipitated asphaltene molecules in the filter membrane images. Higher pressure combined with filter membranes having smaller pore sizes resulted in more asphaltene deposition and pore plugging, as indicated by the darker color in the images. The 50-nm filter paper membrane exhibited darker colors compared to the 450- and 100-nm filters due to the small size of the pores, which led to greater asphaltene deposition.

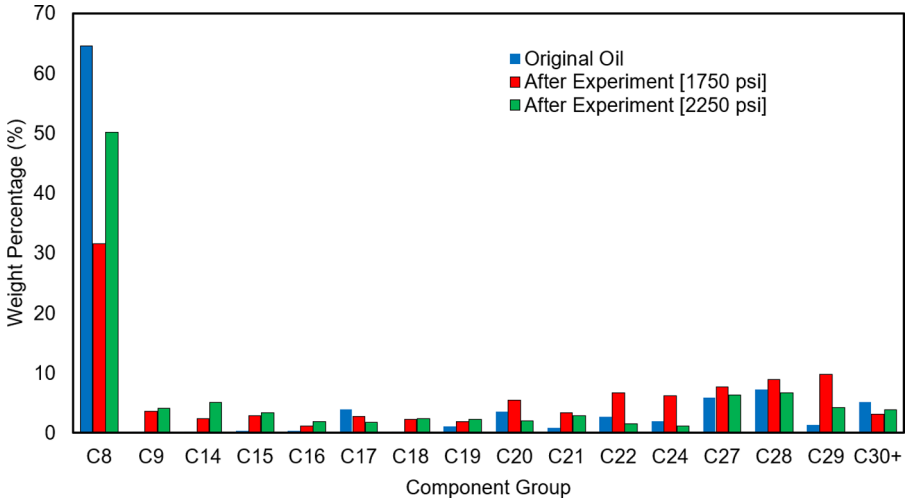

Fig. 18—Distribution of oil components before and after N_2 gas injection filtration experiments at 1,750 and 2,250 psi.

Component Group	Weight Percentage (%)		
	Before Experiment (Original Oil)	After Experiment	
		1,750 psi	2,250 psi
C_1-C_7	0.00	0.00	0.00
C_8-C_{14}	65.14	37.58	59.44
C_{15}-C_{19}	6.06	11.08	11.76
C_{20}-C_{24}	9.16	21.83	7.68
C_{25}-C_{29}	14.48	26.37	17.21
C_{30+} (including asphaltene)	5.17	3.14	3.91
Total	100.00	100.00	100.00

Table 3—Gas chromatography analysis before and after N_2 gas injection filtration experiments at 1,750 and 2,250 psi

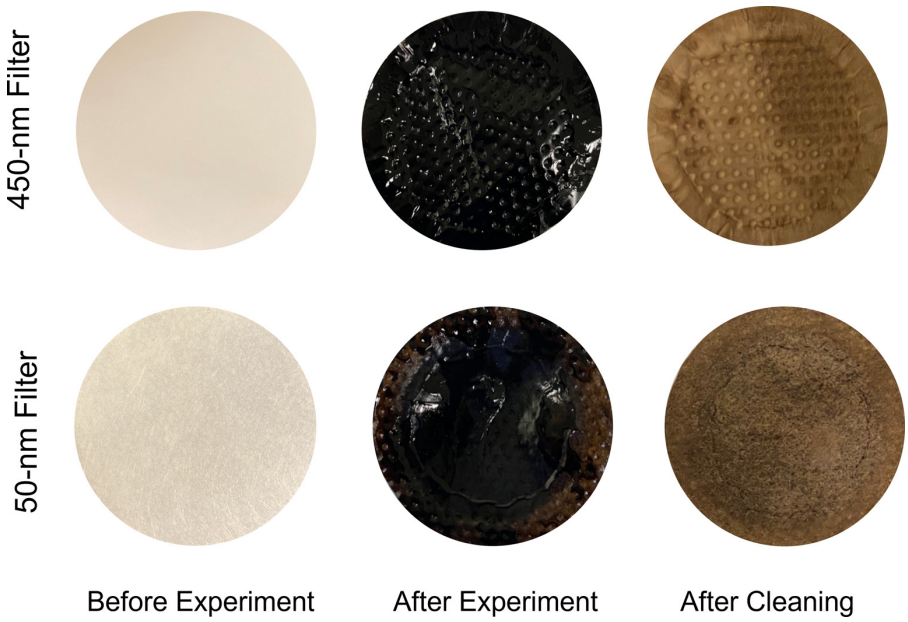

Fig. 19—Illustration of the filter membrane (450 and 50 nm) at 2,000 psi before and after the experiment and after cleaning.

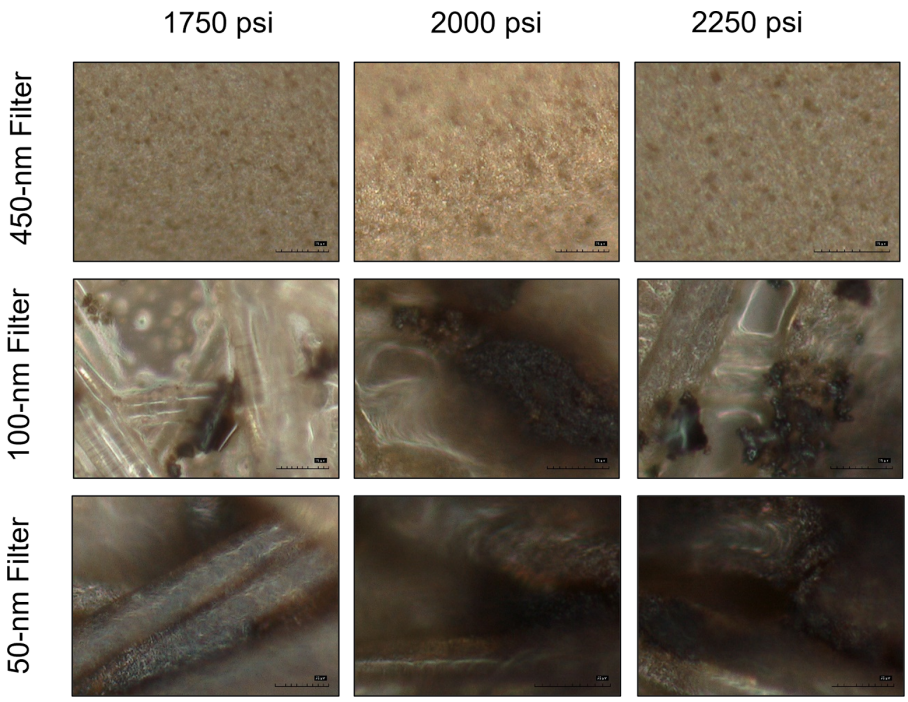

Fig. 20—Digital microscopic images (20 μm) of 450-, 100-, and 50-nm filter membranes using various miscible N_2 injection pressures.

SEM Analysis. SEM provides advanced imaging analysis that can determine the pore structure, particularly in unconventional shale formations, which are known for their small pore sizes. SEM was used to highlight the impact of pressure and asphaltene particles on pore plugging. To illustrate this, a collection of SEM images was taken for all heterogenous filter membranes (450, 100, and 50 nm) during 1,750- and 2,250-psi N_2 injection. **Fig. 21** shows SEM images (5 μm) of the filter membranes' pore structures for 450-, 100-, and 50-nm filters using N_2 injection pressures of 1,750 and 2,250 psi at 32°C. For 450-nm filter paper, the images show asphaltenes accumulated inside the structure, which is colored black, during 1,750- and 2,250-psi injection pressure. The filter paper pore plugging was the most severe in the 50-nm filter membrane using 2,250 psi. Because 450-nm filter has a larger pore size, the imaging clearly captured the structure of the 450-nm filter membranes but not those of the smaller filters. As the pore size of the filter membrane decreased, dark colors were observed for the 100-nm filter membrane. Most of the area of 100-nm filter papers was affected by asphaltene depositions, with the darker color observed at 1,750-psi injection pressure. This confirms that the asphaltenes had a greater impact on the smaller pore structure compared to the 450-nm filter. For the 50-nm filter membranes, most of the photo areas were impacted by asphaltenes due to the smaller pores.

Pore Size Reduction Caused by Asphaltene Deposition. To identify the effect of asphaltene on the pore plugging of the filter paper membranes, the SEM images were processed using computer software to analyze the pore size of each filter membrane. **Fig. 22** compares the pore size distribution in a 450-nm filter membrane after N_2 injections of 1,750 and 2,250 psi. The estimated pore size distribution in a 450-nm filter paper ranged from 40 to 250 nm using 1,750 psi and 50 nm to 180 nm using 2,250 psi. The results showed that the higher pressure (2,250 psi) had a greater impact on pore plugging compared to the lower pressure (1,750 psi). This occurred because the higher pressure had a greater effect on the asphaltene particles and resulted in more asphaltene precipitation and deposition, thus reducing the pore sizes. The oil path in the filter membranes became smaller because of asphaltene deposition and resulted in reductions in the pore sizes in the filter membrane. The same observations were also found in the 100- and 50-nm filter membranes. For the 100-nm filter membrane, the pore size distribution ranged between 10 and 40 nm for the lower pressure (1,750 psi) and between 15 and 35 nm for the higher pressure (2,250 psi), as shown in **Fig. 23.** Smaller pore size distributions were observed in the 50-nm filter membrane due to the smaller size of the pores. The results of the pore size distribution in the 50-nm filter membrane are shown in **Fig. 24.** The asphaltene particles accumulated at higher percentages in the smaller pores of the filter membranes and then plugged most of the pores. Smaller pore size leads to more asphaltene concentration, which leads to more pore plugging. Su et al. (2021) developed an integrated simulation approach to predict permeability reduction under asphaltene particle aggregation and deposition. They concluded that longer aggregation time, higher flow velocity, and bigger precipitation concentrations will lead to a faster reduction in permeability. These results revealed that asphaltenes in crude oil can be induced by N_2 injection and can cause severe pore plugging, especially in reservoirs that have the small pores that are present in unconventional reservoirs.

Miscible vs. Immiscible Discussion. Asphaltene deposition and precipitation during N_2 gas injection is a major problem in enhanced oil recovery projects. Investigation of asphaltene instability in crude oil during miscible and immiscible N_2 gas injection is very important to avoid any future problems such as pore plugging and permeability reduction. In this research, the miscible N_2 gas injection impacted the stability of the asphaltene clusters in the crude oil. To provide a whole picture of the impact of miscible and immiscible N_2 gas injection on asphaltene clusters, the essential results of immiscible N_2 condition from the previous work will be discussed (Elturki and Imqam 2021b). **Fig. 25** shows a comparison of asphaltene weight percent in immiscible (i.e., 1,000, 1,250, and 1,500 psi) and miscible (1,750, 2,000, and 2,250 psi) N_2 injection in 450-, 100-, and 50-nm filter paper membranes. **Table 4** presents the estimated asphaltene weight percentages from different collected areas during immiscible and miscible conditions. The results demonstrated that the asphaltene clusters in the crude oil were induced due to N_2 gas injection in all experiments. When the pressure was lower than the N_2 MMP, a lower average of asphaltene weight percent was observed compared to miscible conditions. Once the pressure exceeded the MMP, the asphaltene weight percent increased significantly in all filter membranes, especially in smaller pore size structures (i.e., 50

nm). More oil was produced during higher pressures, and thus more asphaltene weight percent was determined. Smaller pore size structure led to higher asphaltene percentages. These observations confirm that during miscible gas injection of N_2, higher oil recovery is expected with more asphaltene issues during production processes. The N_2 evaporation during pressures less than MMP improves the crude oil capability to overcome the asphaltene clusters' breakdown. During miscible conditions, the connection between asphaltenes and resins in the crude oil becomes much weaker and leads to a higher rate of asphaltene deposition and fluctuation. As a result, asphaltene aggregation and fluctuation during immiscible N_2 injection would not be challenging in the enhanced oil recovery process as miscible N_2 injection.

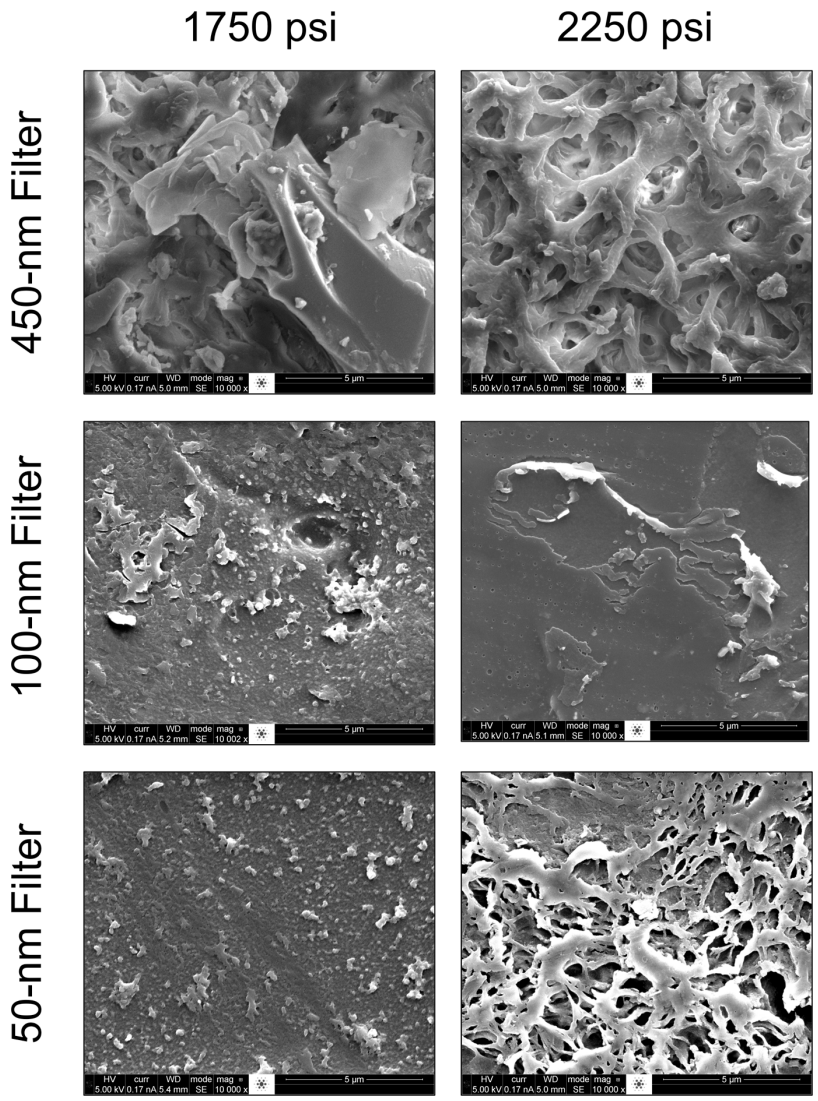

Fig. 21—SEM images (5 μm) of 450-, 100-, and 50-nm filter membranes at 1,750- and 2,250-psi injection pressures.

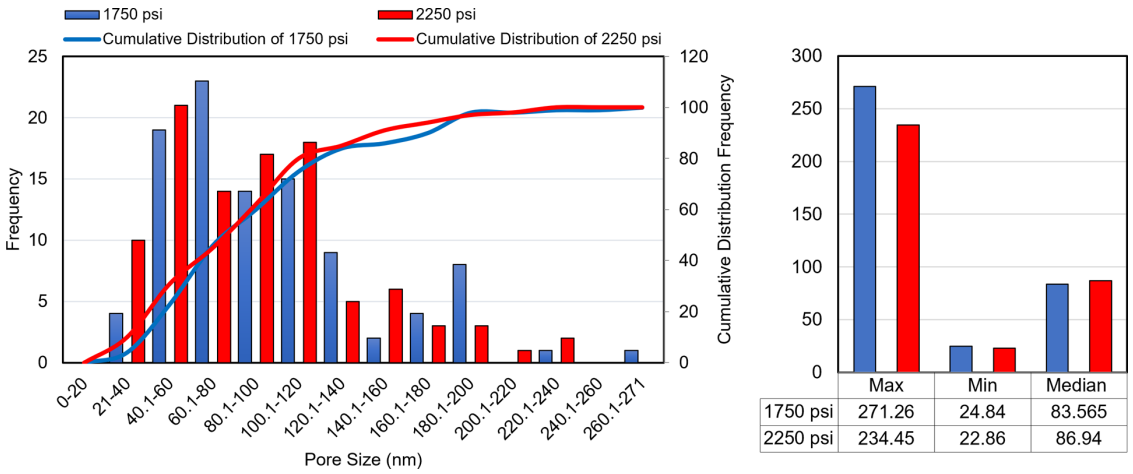

	Max	Min	Median
1750 psi	271.26	24.84	83.565
2250 psi	234.45	22.86	86.94

Fig. 22—Comparison of the estimated pore size distribution in a 450-nm filter membrane after N_2 injections at 1,750 and 2,250 psi.

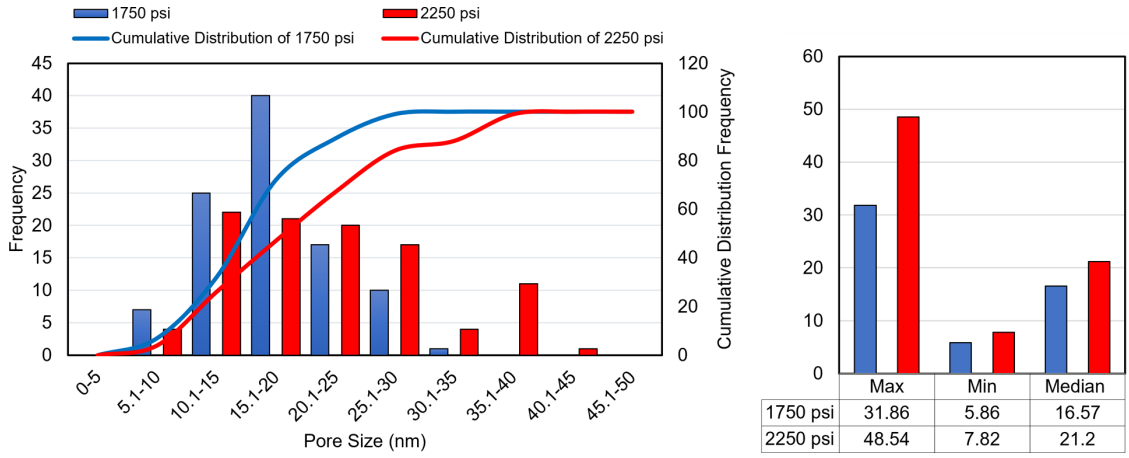

Fig. 23—Comparison of the estimated pore size distribution in a 100-nm filter membrane after N_2 injections at 1,750 and 2,250 psi.

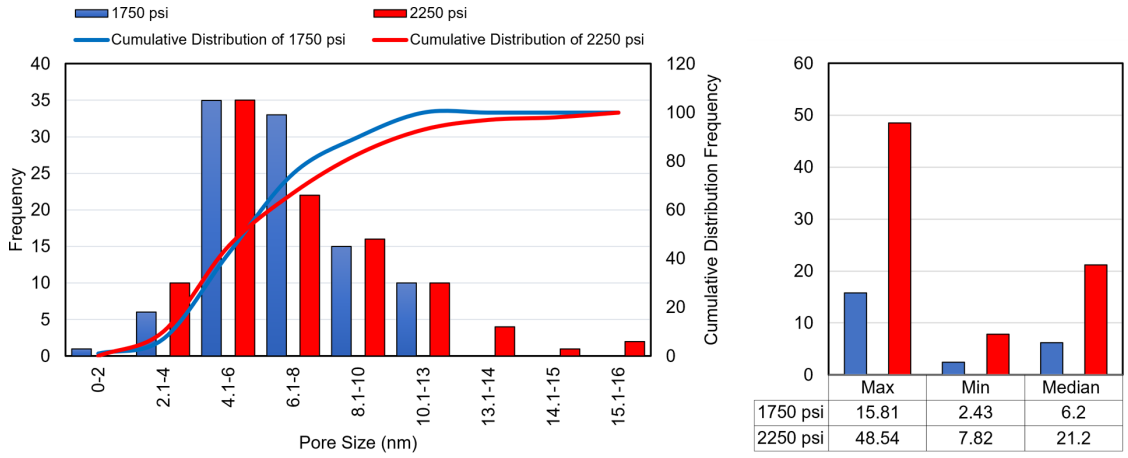

Fig. 24—Comparison of the estimated pore size distribution in a 50-nm filter membrane after N_2 injections at 1,750 and 2,250 psi.

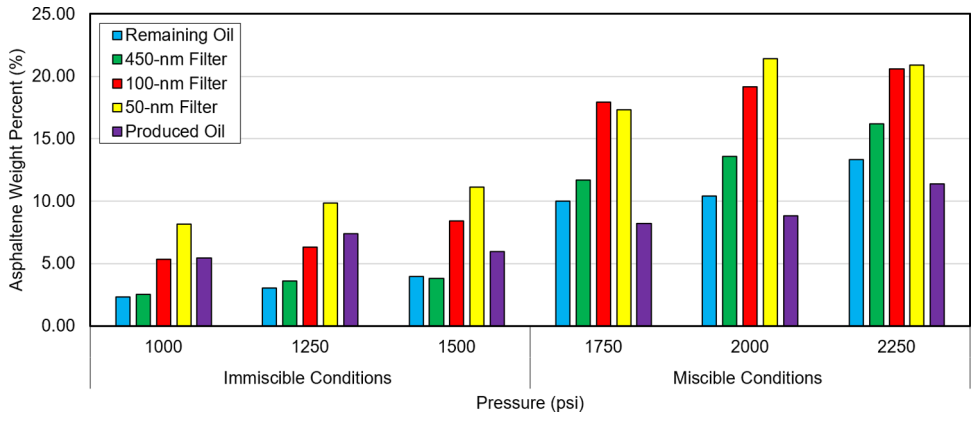

Fig. 25—Comparison of asphaltene weight percentages during immiscible (Elturki and Imqam 2021b) and miscible N_2 injection.

Collected Oil Area	Asphaltene Weight (%)					
	Immiscible Pressure			Miscible Pressure		
	1,000 psi	1,250 psi	1,500 psi	1,750 psi	2,000 psi	2,250 psi
Remaining oil	2.30	3.04	3.96	10.00	10.42	13.33
450-nm filter	2.52	3.61	3.81	11.67	13.56	16.18
100-nm filter	5.36	6.30	8.40	17.91	19.18	20.59
50-nm filter	8.14	9.83	11.11	17.33	21.43	20.90
Produced oil	5.46	7.39	5.95	8.20	8.82	11.36

Table 4—Estimated asphaltene weight percentages from different collected areas during immiscible and miscible conditions.

Conclusions

This research implemented three sets of experiments to investigate asphaltene stability under miscible N_2 injection pressure. First, the MMP of N_2 was determined using a slimtube. Then, filtration and visualization asphaltene experiments were conducted. The following factors were investigated: injection pressure, temperature, mixing time, filter membrane heterogeneity, and different pore sizes. Based on the results, we suggest the following conclusions:

- The asphaltene weight percent increased as the N_2 injection pressure increased in all the filtration experiments because the higher pressure weakened the bonds between the resins and asphaltenes, which led to asphaltene deposition.
- At higher temperatures, the precipitated asphaltenes that formed from the colloidal suspension particles tended to dissolve in the oil; thus, more asphaltenes will form in a soluble condition, but fewer will form under colloidal conditions.
- When using a heterogeneous distribution of filter sizes (i.e., 450, 100, and 50 nm) and as the pore size decreased, the asphaltene weight percent increased because the asphaltene clusters were unable to pass easily through the smaller pores of the filter membranes.
- Using a uniform pore size distribution inside the vessel (100 nm) resulted in almost the same asphaltene weight percent as the heterogeneous distribution because of the size of the asphaltene particles that passed through all of the same pore size filter membranes. Additionally, increasing the mixing time produced a higher asphaltene weight percent.
- The chromatography results demonstrated that the weight percent of the heavy components, including asphaltene, was higher when using 1,750 psi than when using 2,250 psi.
- The microscopy imaging illustrated the severity of the asphaltene deposition on pore plugging. The results showed an increase in pore plugging when the pressure increased coupled with a decrease in the pore size.
- SEM showed how the asphaltene particles affected the pore plugging: At a higher pressure and with a smaller pore size, the asphaltene particles caused more severe pore plugging.
- Pore size distribution analysis showed that the pore size decreased significantly in all the filter paper membranes due to asphaltene plugging.

Acknowledgments

The authors acknowledge the National Science Foundation chemical, biological, environmental, and transport systems for funding the work under Grant CBET-1932965.

References

Afra, S., Samouei, H., Golshahi, N. et al. 2020. Alterations of Asphaltenes Chemical Structure Due to Carbon Dioxide Injection. *Fuel* **272:** 117708. https://doi.org/10.1016/j.fuel.2020.117708.

Ali, S. I., Lalji, S. M., Haneef, J. et al. 2021. Critical Analysis of Different Techniques Used To Screen Asphaltene Stability in Crude Oils. *Fuel* **299:** 120874. https://doi.org/10.1016/j.fuel.2021.120874.

Alimohammadi, S., Sayyad Amin, J., and Nikooee, E. 2017. Estimation of Asphaltene Precipitation in Light, Medium and Heavy Oils: Experimental Study and Neural Network Modeling. *Neural Comput Applic* **28** (4): 679–694. https://doi.org/10.1007/s00521-015-2097-3.

Altawati, F., Sheng, J., and Emadi, H. 2020. Investigating Effects of Water on Shale Oil Formation by Using Cyclic Gas Injection Technique: An Experimental Study. Paper presented at the 54th US Rock Mechanics/Geomechanics Symposium, physical event cancelled, 28 June–1 July. ARMA-2020-1054.

Alves, C. A., Romero Yanes, J. F., Feitosa, F. X. et al. 2019. Effect of Temperature on Asphaltenes Precipitation: Direct and Indirect Analyses and Phase Equilibrium Study. *Energy Fuels* **33** (8): 6921–6928. https://doi.org/10.1021/acs.energyfuels.9b00408.

Bahman, J., Nasiri, M., Sabeti, M. et al. 2017. An Introduction to Asphaltenes Chemistry. In *Heavy Oil: Characteristics, Production and Emerging Technologies*, Vol. 93, Chapter 5. Hauppauge, New York, USA: Nova Science Publishers.

Belhaj, H., Abu Khalifeh, H. A., and Javid, K. 2013. Potential of Nitrogen Gas Miscible Injection in South East Assets, Abu Dhabi. Paper presented at the North Africa Technical Conference and Exhibition, Cairo, Egypt, 15–17 April. SPE-164774-MS. https://doi.org/10.2118/164774-MS.

Biheri, G. and Imqam, A. 2020. Proppant Transport by High Viscosity Friction Reducer and Guar Linear Gel-Based Fracture Fluids. Paper presented at the 54th US Rock Mechanics/Geomechanics Symposium, physical event cancelled, 28 Jun–1 July. ARMA-2020-1221.

Biheri, G. and Imqam, A. 2021a. Settling of Spherical Particles in High Viscosity Friction Reducer Fracture Fluids. *Energies* **14** (9): 2462. https://doi.org/10.3390/en14092462.

Biheri, G. and Imqam, A. 2021b. Proppant Transport Using High Viscosity Friction Reducer Fracture Fluids at High-Temperature Environment. *SPE J*. SPE-206750-PA (in press; posted 26 October 2021). https://doi.org/10.2118/206750-PA.

Branco, V. A. M., Mansoori, G. A., Xavier, L. C. D. A. et al. 2001. Asphaltene Flocculation and Collapse from Petroleum Fluids. *J Pet Sci Eng* **32** (2–4): 217–230. https://doi.org/10.1016/S0920-4105(01)00163-2.

Buriro, M. A. and Shuker, M. T. 2012. Asphaltene Prediction and Prevention: A Strategy To Control Asphaltene Precipitation. Paper presented at the SPE/PAPG Annual Technical Conference, Islamabad, Pakistan, 3–5 December. SPE-163129-MS. https://doi.org/10.2118/163129-MS.

Buriro, M. A. and Shuker, M. T. 2013. Minimizing Asphaltene Precipitation in Malaysian Reservoir. Paper presented at the SPE Saudi Arabia Section Technical Symposium and Exhibition, Al-Khobar, Saudi Arabia, 19–22 May. SPE-168105-MS. https://doi.org/10.2118/168105-MS.

Chandio, Z. A., Ramasamy, M., and Mukhtar, H. B. 2015. Temperature Effects on Solubility of Asphaltenes in Crude Oils. *Chem Eng Res Des* **94:** 573–583. https://doi.org/10.1016/j.cherd.2014.09.018.

Chung, T. H. 1992. Thermodynamic Modeling for Organic Solid Precipitation. Paper presented at the SPE Annual Technical Conference and Exhibition, Washington, DC, USA, 4–7 October. SPE-24851-MS. https://doi.org/10.2118/24851-MS.

Elturki, M. and Imqam, A. 2020a. Application of Enhanced Oil Recovery Methods in Unconventional Reservoirs: A Review and Data Analysis. Paper presented at the 54th US Rock Mechanics/Geomechanics Symposium, physical event cancelled, 28 June–1 July. ARMA-2020-1081.

Elturki, M. and Imqam, A. 2020b. High Pressure-High Temperature Nitrogen Interaction with Crude Oil and Its Impact on Asphaltene Deposition in Nano Shale Pore Structure: An Experimental Study. Paper presented at the SPE/AAPG/SEG Unconventional Resources Technology Conference, Virtual, 20–22 July. URTEC-2020-3241-MS. https://doi.org/10.15530/urtec-2020-3241.

Elturki, M. and Imqam, M. 2021a. Analysis of Nitrogen Minimum Miscibility Pressure (MMP) and Its Impact on Instability of Asphaltene Aggregates: An Experimental Study. Paper presented at the SPE Trinidad and Tobago Section Energy Resources Conference, Virtual, 28–30 June. SPE-200900-MS. https://doi.org/10.2118/200900-MS.

Elturki, M. and Imqam, A. 2021b. Asphaltene Thermodynamic Flocculation during Immiscible Nitrogen Gas Injection. *SPE J*. **26** (5): 3188–3204. SPE-206709-PA. https://doi.org/10.2118/206709-PA.

Elturki, M., McElroy, P. D., Li, D. et al. 2021. Simulation Study Investigating the Impact of Carbon Dioxide Foam Fracturing Fluids on Proppant Transport. Paper presented at the SPE Trinidad and Tobago Section Energy Resources Conference, Virtual, 28– 30 June. SPE-200950-MS. https://doi.org/10.2118/200950-MS.

Elwegaa, K. and Emadi, H. 2019. Improving Oil Recovery from Shale Oil Reservoirs Using Cyclic Cold Nitrogen Injection–An Experimental Study. *Fuel* **254:** 115716. https://doi.org/10.1016/j.fuel.2019.115716.

Fakher, S. 2020. *Investigating the Factors Impacting the Success of Immiscible Carbon Dioxide Injection in Unconventional Shale Reservoirs: An Experimental Study*. PhD dissertation, Missouri University of Science and Technology, Rolla, Missouri, USA.

Fakher, S. and Imqam, A. 2019. Asphaltene Precipitation and Deposition during CO_2 Injection in Nano Shale Pore Structure and Its Impact on Oil Recovery. *Fuel* **237:** 1029–1039. https://doi.org/10.1016/j.fuel.2018.10.039.

Fakher, S. and Imqam, A. 2020. An Experimental Investigation of Immiscible Carbon Dioxide Interactions with Crude Oil: Oil Swelling and Asphaltene Agitation. *Fuel* **269:** 117380. https://doi.org/10.1016/j.fuel.2020.117380.

Goual, L. 2012. Petroleum Asphaltenes. In *Crude Oil Emulsions-Composition Stability and Characterization*, ed. A.-R. M. El-Sayed. London, England, UK: InTech Open. https://doi.org/10.5772/35875.

Hassanpouryouzband, A., Joonaki, E., Taghikhani, V. et al. 2018a. New Two-Dimensional Particle-Scale Model To Simulate Asphaltene Deposition in Wellbores and Pipelines. *Energy Fuels* **32** (3): 2661–2672. https://doi.org/10.1021/acs.energyfuels.7b02714.

Hassanpouryouzband, A., Joonaki, E., Vasheghani Farahani, M. et al. 2020. Gas Hydrates in Sustainable Chemistry. *Chem Soc Rev* **49** (15): 5225–5309. https://doi.org/10.1039/C8CS00989A.

Hassanpouryouzband, A., Yang, J., Tohidi, B. et al. 2018b. CO_2 Capture by Injection of Flue Gas or CO_2-N_2 Mixtures into Hydrate Reservoirs: Dependence of CO_2 Capture Efficiency on Gas Hydrate Reservoir Conditions. *Environ Sci Technol* **52** (7): 4324–4330. https://doi.org/10.1021/acs.est.7b05784.

Hassanpouryouzband, A., Yang, J., Tohidi, B. et al. 2019. Geological CO_2 Capture and Storage with Flue Gas Hydrate Formation in Frozen and Unfrozen Sediments: Method Development, Real Time-Scale Kinetic Characteristics, Efficiency, and Clathrate Structural Transition. *ACS Sustain Chem Eng* **7** (5): 5338–5345. https://doi.org/10.1021/acssuschemeng.8b06374.

Hoepfner, M. P., Limsakoune, V., Chuenmeechao, V. et al. 2013. A Fundamental Study of Asphaltene Deposition. *Energy & Fuels* **27** (2): 725–735. https://doi.org/10.1021/ef3017392.

Jamaluddin, A. K. M., Joshi, N., Iwere, F. et al. 2002. An Investigation of Asphaltene Instability under Nitrogen Injection. Paper presented at the SPE International Petroleum Conference and Exhibition in Mexico, Villahermosa, Mexico, 10–12 February. SPE-74393-MS. https://doi.org/10.2118/74393-MS.

Kar, T., Naderi, K., and Firoozabadi, A. 2020. Asphaltene Deposition and Removal in Flowlines and Mitigation by Effective Functional Molecules. *SPE J.* **25** (2): 771–787. SPE-199878-PA. https://doi.org/10.2118/199878-PA.

Mahdaviara, M., Amar, M. N., Hemmati-Sarapardeh, A. et al. 2021. Toward Smart Schemes for Modeling CO_2 Solubility in Crude Oil: Application to Carbon Dioxide Enhanced Oil Recovery. *Fuel* **285:** 119147. https://doi.org/10.1016/j.fuel.2020.119147.

Moradi, S., Dabiri, M., Dabir, B. et al. 2012b. Investigation of Asphaltene Precipitation in Miscible Gas Injection Processes: Experimental Study and Modeling. *Braz J Chem Eng* **29** (3): 665–676. https://doi.org/10.1590/S0104-66322012000300022.

Moradi, S., Dabir, B., Rashtchian, D. et al. 2012a. Effect of Miscible Nitrogen Injection on Instability, Particle Size Distribution, and Fractal Structure of Asphaltene Aggregates. *J Dispers Sci Technol* **33** (5): 763–770. https://doi.org/10.1080/01932691.2011.567878.

Mozaffari, S., Tchoukov, P., Atias, J. et al. 2015. Effect of Asphaltene Aggregation on Rheological Properties of Diluted Athabasca Bitumen. *Energy & Fuels* **29** (9): 5595–5599. https://doi.org/10.1021/acs.energyfuels.5b00918.

Nguyen, T. A. and Ali, S. M. 1998. Effect of Nitrogen on the Solubility and Diffusivity of Carbon Dioxide into Oil and Oil Recovery by the Immiscible WAG Process. *J Can Pet Technol* **37** (2): 24–31. PETSOC-98-02-02. https://doi.org/10.2118/98-02-02.

Pereira, J. C., Lœpez, I., Salas, R. et al. 2007. Resins: The Molecules Responsible for the Stability/Instability Phenomena of Asphaltenes. *Energy & Fuels* **21** (3): 1317–1321. https://doi.org/10.1021/ef0603333.

Rashid, Z., Wilfred, C. D., Gnanasundaram, N. et al. 2019. A Comprehensive Review on the Recent Advances on the Petroleum Asphaltene Aggregation. *J Pet Sci Eng* **176:** 249–268. https://doi.org/10.1016/j.petrol.2019.01.004.

Rostami, A., Arabloo, M., Kamari, A. et al. 2017. Modeling of CO_2 Solubility in Crude Oil during Carbon Dioxide Enhanced Oil Recovery Using Gene Expression Programming. *Fuel* **210:** 768–782. https://doi.org/10.1016/j.fuel.2017.08.110.

Sebastian, H. M. and Lawrence, D. D. 1992. Nitrogen Minimum Miscibility Pressures. Paper presented at the SPE/DOE Enhanced Oil Recovery Symposium, Tulsa, Oklahoma, USA, 22–24 April. SPE-24134-MS. https://doi.org/10.2118/24134-MS.

Shen, Z. and Sheng, J. J. 2017. Experimental Study of Permeability Reduction and Pore Size Distribution Change Due to Asphaltene Deposition during CO_2 Huff and Puff Injection in Eagle Ford Shale. *Asia Pac J Chem Eng* **12** (3): 381–390. https://doi.org/10.1002/apj.2080.

Shen, Z. and Sheng, J. J. 2018. Experimental and Numerical Study of Permeability Reduction Caused by Asphaltene Precipitation and Deposition during CO_2 Huff and Puff Injection in Eagle Ford Shale. *Fuel* **211:** 432–445. https://doi.org/10.1016/j.fuel.2017.09.047.

Shi, B., Song, S., Chen, Y. et al. 2021. Status of Natural Gas Hydrate Flow Assurance Research in China: A Review. *Energy Fuels* **35** (5): 3611–3658. https://doi.org/10.1021/acs.energyfuels.0c04209.

Soroush, S., Pourafshary, P., and Vafaie-Sefti, M. 2014. A Comparison of Asphaltene Deposition in Miscible and Immiscible Carbon Dioxide Flooding in Porous Media. Paper presented at the SPE EOR Conference at Oil and Gas West Asia, Muscat, Oman, 31 March–2 April. SPE-169657-MS. https://doi.org/10.2118/169657-MS.

Srivastava, R. K. and Huang, S. S. 1997. Asphaltene Deposition during CO_2 Flooding: A Laboratory Assessment. Paper presented at the SPE Production Operations Symposium, Oklahoma City, Oklahoma, USA, 9–11 March. SPE-37468-MS. https://doi.org/10.2118/37468-MS.

Su, X., Moghanloo, R. G., Qi, M. et al. 2021. An Integrated Simulation Approach To Predict Permeability Impairment under Simultaneous Aggregation and Deposition of Asphaltene Particles. *SPE J.* **26** (2): 959–972. SPE-205028-PA. https://doi.org/10.2118/205028-PA.

Vahidi, A. and Zargar, G. 2007. Sensitivity Analysis of Important Parameters Affecting Minimum Miscibility Pressure (MMP) of Nitrogen Injection into Conventional Oil Reservoirs. Paper presented at the SPE/EAGE Reservoir Characterization and Simulation Conference, Abu Dhabi, UAE, 28–31 October. SPE-111411-MS. https://doi.org/10.2118/111411-MS.

Wang, P., Zhao, F., Hou, J. et al. 2018. Comparative Analysis of CO_2, N_2, and Gas Mixture Injection on Asphaltene Deposition Pressure in Reservoir Conditions. *Energies* **11** (9): 2483. https://doi.org/10.3390/en11092483.